

# Cationic Arylmanganese(II) Derivatives Occurring in Ion-Pair Forms with Tetraphenylborate Anions: Synthetic, Structural, and Magnetic Studies

Euro Solari, Fabrizio Musso, Emma Gallo, and Carlo Floriani\*<sup>1</sup>

*Institut de Chimie Minérale et Analytique, BCH, Université de Lausanne, CH-1015 Lausanne, Switzerland*

Nazzareno Re

*Dipartimento di Chimica, Università di Perugia, I-06100 Perugia, Italy*

Angiola Chiesi-Villa and Corrado Rizzoli

*Dipartimento di Chimica, Università di Parma, I-43100 Parma, Italy*

Received December 21, 1994<sup>®</sup>

We report a class of cationic manganese(II) aryl compounds stabilized by weak donor solvents or by interactions with the counteranion  $\text{BPh}_4^-$  to form ion-pair species. The parent compound used was  $\text{Mn}_3\text{Mes}_6$  (**1**; Mes = 2,4,6-Me<sub>3</sub>C<sub>6</sub>H<sub>2</sub>), which can be synthesized on a large scale by a conventional method and conveniently used as starting material. Reaction of **1** with  $\text{BPh}_3$  in  $\text{Et}_2\text{O}$  gave the cationic derivative  $[\text{MesMn}(\text{OEt}_2)_3]^+\text{BPh}_4^-$  (**2**), containing a single Mn–C bond and three weakly bonded  $\text{Et}_2\text{O}$  molecules. In order to avoid coordinating solvent, the reaction between **1** and  $\text{BPh}_3$  was then carried out in toluene. This reaction gave, depending on the reaction time and the  $\text{BPh}_3/\text{Mn}$  ratio, the monomeric  $[\text{MesMn}(\eta^3\text{-Ph})_2\text{-BPh}_2]$  (**3**) and the dimeric  $[\text{Ph}_2\text{B}(\eta^2\text{-Ph})_2(\mu\text{-MnPh})_2(\eta^2\text{-Ph})_2\text{BPh}_2]$  (**4**) ion pairs. Temperature-dependent magnetic measurements showed that for **1** and **4** a strong antiferromagnetic coupling exists between the  $d^5$  ions brought about by the bridging aryl groups and/or the short Mn··Mn distance (2.851(2) Å, **1**; 2.796(1) Å, **4**). Such a coupling, much greater than that observed in several Mn(II)–Mn(II) dimers, has  $J$  values of 55.4  $\text{cm}^{-1}$  (complex **4**) and 40.4  $\text{cm}^{-1}$  (complex **1**). Crystallographic details: **1** is triclinic, space group  $P\bar{1}$ , with  $a = 12.850(3)$  Å,  $b = 20.327(4)$  Å,  $c = 11.407(3)$  Å,  $\alpha = 95.11(2)^\circ$ ,  $\beta = 114.00(2)^\circ$ ,  $\gamma = 98.77(2)^\circ$ ,  $Z = 2$ , and  $R = 0.052$ ; **2** is triclinic, space group  $P\bar{1}$ , with  $a = 11.237(2)$  Å,  $b = 19.035(2)$  Å,  $c = 10.991(1)$  Å,  $\alpha = 99.30(1)^\circ$ ,  $\beta = 106.66(1)^\circ$ ,  $\gamma = 104.58(1)^\circ$ ,  $Z = 2$ , and  $R = 0.070$ ; **3** is monoclinic, space group  $P2_1/n$ , with  $a = 10.070(1)$  Å,  $b = 15.901(1)$  Å,  $c = 20.876(2)$  Å,  $\beta = 101.94(1)^\circ$ ,  $Z = 4$ , and  $R = 0.054$ ; **4** is monoclinic, space group  $P2_1/c$ , with  $a = 15.074(4)$  Å,  $b = 13.289(4)$  Å,  $c = 20.139(5)$  Å,  $\beta = 98.39(2)^\circ$ ,  $Z = 4$ , and  $R = 0.055$ .

## Introduction

The organometallic and coordination chemistry of manganese has undergone a renaissance due to the role of this metal in a number of naturally occurring systems,<sup>2</sup> in very efficient catalytic oxidation systems,<sup>3</sup> and, to a lesser extent, in organometallic chemistry.<sup>4</sup> The major objectives of the last class have essentially been focused on (i) the *in situ* synthesis of the Mn–C

functionality with the aim of exploiting it in organic synthesis<sup>4</sup> and (ii) the stabilization of complexes with Mn–C functionalities. The organometallic complexes of manganese which have attracted the most attention in recent years are the homoleptic alkyl and aryl derivatives.<sup>5</sup> A quite successful strategy, which has been applied mainly to zirconium organometallics, has been the generation of coordinatively unsaturated species in the form of cationic alkyls, having Lewis acid properties.<sup>6–8</sup> Although the homoleptic alkyl or aryl complexes of manganese are very reactive, one synthetic challenge would be the generation of cationic analogues for their utilization in catalysis.<sup>6</sup> In addition, with particular regard to the preparation of manganese organometallics, *in situ*,<sup>4</sup> we feel that under some of the

<sup>®</sup> Abstract published in *Advance ACS Abstracts*, April 15, 1995.

(1) To whom correspondence should be addressed.

(2) (a) *Manganese Redox Enzymes*; Pecoraro, V. L., Ed.; VCH: New York, 1992. (b) Wiegand, K. *Angew. Chem., Int. Ed. Engl.* **1989**, *28*, 1153. (c) Pecoraro, V. L.; Baldwin, M. J.; Gelasco, A. *Chem. Rev.* **1994**, *94*, 807.

(3) (a) Srinivasan, K.; Michaud, P.; Kochi, J. K. *J. Am. Chem. Soc.* **1986**, *108*, 2309. (b) Menage, S.; Collomb-Dunand Sauthier, M. N.; Lambeaux, C.; Fontecave, M. *J. Chem. Soc., Chem. Commun.* **1994**, 1885. (c) Eilmes, J. *Polyhedron* **1992**, *11*, 581. (d) O'Connor, K. J.; Wey, S. J.; Burrows, C. J. *Tetrahedron Lett.* **1992**, *33*, 1001. (e) Evans, D. A.; Faul, M. M.; Bilodeau, M. T.; Anderson, B. A.; Barnes, D. M. *J. Am. Chem. Soc.* **1993**, *115*, 5328. (f) Reddy, D. R.; Thornton, E. R. *J. Chem. Soc., Chem. Commun.* **1992**, 172. (g) Zhang, W.; Jacobsen, E. N. *J. Org. Chem.* **1991**, *56*, 2296. (h) Jacobsen, E. N.; Zhang, W.; Muci, A. R.; Ecker, J. R.; Deng, L. *J. Am. Chem. Soc.* **1991**, *113*, 7063. (i) Larrow, J. F.; Jacobsen, E. N. *J. Org. Chem.* **1994**, *59*, 1939. (j) Brandes, B. D.; Jacobsen, E. N. *J. Org. Chem.* **1994**, *59*, 4378.

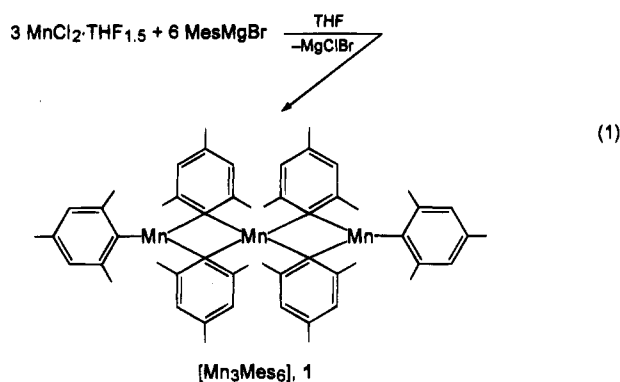
(4) (a) Normant, J. F.; Cahiez, G. In *Modern Synthetic Methods*; Scheffold, R., Ed.; Wiley: Chichester, U.K., 1983; Vol. 3, p 173. (b) Cahiez, G.; Alami, M. *Tetrahedron* **1989**, *45*, 4163. (c) Cahiez, G.; Marquis, S. *Synlett* **1993**, 45. (d) Cahiez, G.; Figadere, B.; Clery, P. *Tetrahedron Lett.* **1994**, *35*, 3065. (e) Cahiez, G.; Chau, K.; Clery, P. *Tetrahedron Lett.* **1994**, *35*, 3069. (f) Corey, E. J.; Posner, G. H. *Tetrahedron Lett.* **1970**, 315. (g) Reetz, M. T.; Haning, H. *Tetrahedron Lett.* **1993**, *34*, 7395. (h) Reetz, M. T.; Haning, H.; Stanchev, S. *Tetrahedron Lett.* **1992**, *33*, 6963. (i) Reetz, M. T.; Rölfling, K.; Griebenow, N. *Tetrahedron Lett.* **1994**, *35*, 1969.

reaction conditions employed, the protolysis or ionization of the Mn–C bond can occur, with the consequent formation of cationic species. Among the various strategies used for that purpose,<sup>6–8</sup> i.e. controlled protolysis or reaction with a Lewis acid, the latter one is preferred since the resulting cation can be generated under noncoordinating conditions.

This report concerns the synthesis and structural characterization of the parent compound [Mn<sub>3</sub>Mes<sub>6</sub>], which has been previously communicated,<sup>5h</sup> and its conversion into masked cationic forms of the [Mn–Ar]<sup>+</sup> fragment by the use of BPh<sub>3</sub>. Such compounds have been isolated as monomers or dimers in the ion-pair form, with BPh<sub>4</sub><sup>–</sup> as the counteranion. A magnetic study on the monomer, dimer, and trimer of this series completes our investigation.

## Results and Discussion

**Synthesis of Cationic Arylmanganese Derivatives.** The synthesis of **1** has been performed by following the conventional method outlined in eq 1.



Complex **1** is usually recrystallized from toluene and contains solvent of crystallization. The successful isolation of **1** in a pure form (without traces of chloride ions) requires a number of precautions, especially when the synthesis is carried out on a large scale. The use of very pure, crystalline MnCl<sub>2</sub>·1.5THF is compulsory, as is the recrystallization of the crude product, at least twice, from toluene. Polynuclear structures such as **1** containing bridging hydrocarbyl ligands are not unusual in the organometallic chemistry of manganese.<sup>4</sup> In contrast

(5) (a) Andersen, R. A.; Carmona-Guzman, E.; Gibson, J. F.; Wilkinson, G. *J. Chem. Soc., Dalton Trans.* **1976**, 2204. (b) Howard, C. G.; Wilkinson, G.; Thornton-Pett, M.; Hursthouse, M. B. *J. Chem. Soc., Dalton Trans.* **1983**, 2025. (c) Howard, C. G.; Girolami, G. S.; Wilkinson, G.; Thornton-Pett, M.; Hursthouse, M. B. *J. Chem. Soc., Dalton Trans.* **1983**, 2631. (d) Girolami, G. S.; Wilkinson, G.; Thornton-Pett, M.; Hursthouse, M. B. *J. Am. Chem. Soc.* **1983**, *105*, 6752. (e) Belforte, A.; Calderazzo, F.; Englert, U.; Strähle, J.; Wurst, K. *J. Chem. Soc., Dalton Trans.* **1991**, 2419. (f) Bartlett, R. A.; Olmstead, M. M.; Power, P. P.; Shoner, S. C. *Organometallics* **1988**, *7*, 1801. (g) Morris, R. J.; Girolami, G. S. *Organometallics* **1991**, *10*, 792, 799. (h) Gambarotta, S.; Floriani, C.; Chiesi-Villa, A.; Guastini, C. *J. Chem. Soc., Chem. Commun.* **1983**, 1128.

(6) Collins, S.; Kuntz, B. A.; Collins, S. *J. Org. Chem.* **1989**, *54*, 4154. Jordan, R. F. *Adv. Organomet. Chem.* **1991**, *32*, 325. Grossman, R. B.; Davis, W. M.; Buchwald, S. L. *J. Am. Chem. Soc.* **1991**, *113*, 2321. Guram, A. S.; Swenson, D. C.; Jordan, R. F. *J. Am. Chem. Soc.* **1992**, *114*, 8991. Guram, A. S.; Guo, Z.; Jordan, R. F. *J. Am. Chem. Soc.* **1993**, *115*, 4902. Guram, A. S.; Jordan, R. F. *J. Org. Chem.* **1993**, *58*, 5595. Hong, Y.; Kuntz, B. A.; Collins, S. *Organometallics* **1993**, *12*, 964.

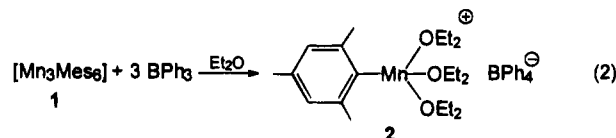
(7) Pino, P.; Cioni, P.; Wei, J. *J. Am. Chem. Soc.* **1987**, *109*, 6189. Waymouth, R. M.; Pino, P. *J. Am. Chem. Soc.* **1990**, *112*, 4911. Morken, J. P.; Didiuk, M. T.; Hoveyda, A. H. *J. Am. Chem. Soc.* **1993**, *115*, 6997. Rodewald, S.; Jordan, R. F. *J. Am. Chem. Soc.* **1994**, *116*, 4491 and references therein.

to these examples, however, **1** can be produced in a large quantity and represents a very useful starting material for the metalation of active proton-containing substrates.<sup>9</sup>

The trimeric structure proposed for **1** is based on the solid-state X-ray analysis. In the presence of even weakly coordinating solvents, such as aromatic hydrocarbons, we expect a breakdown of the structure with a significant interaction of the arenes with the manganese ion. At present, much more attention has been devoted to the weakly stabilized, rather than to the ligand overstabilized, forms of organometallics. A general method which has been successfully used for this type of stabilization is the induced ionization of a metal–aryl bond by an appropriate Lewis acid such as B(C<sub>6</sub>F<sub>5</sub>)<sub>3</sub>.<sup>10</sup> This procedure has been employed mainly in the case of cyclopentadienylmetal alkyl derivatives but not for homoleptic metal alkyl compounds. The organometallic cations thus formed showed a very high reactivity.<sup>6–8</sup>

The reaction of **1** has been studied with a relatively weak Lewis acid, BPh<sub>3</sub>, under various conditions. Initial attempts were carried out in weakly binding solvents such as Et<sub>2</sub>O.

Reaction 2 produces a weakly solvated form of the [Mn–Mes]<sup>+</sup> functionality with the BPh<sub>4</sub><sup>–</sup> counteranion, instead of the expected MesBPh<sub>3</sub><sup>–</sup> anion. Analyzing the

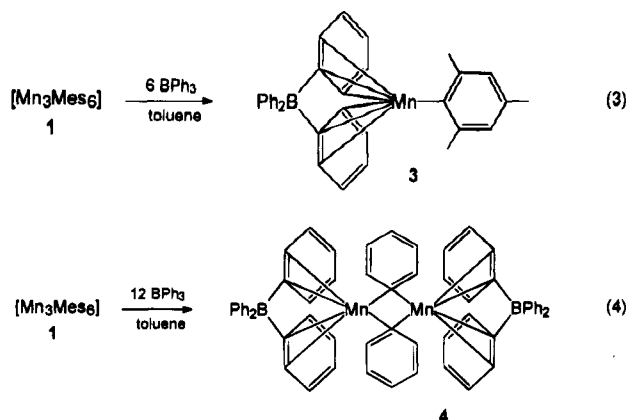


mother liquor of reaction 2 helped us identify MesBPh<sub>2</sub> as a major component. We assume that aryl scrambling occurs between BPh<sub>3</sub> and MesBPh<sub>3</sub><sup>–</sup>, leading preferentially to BPh<sub>4</sub><sup>–</sup> and the identified MesBPh<sub>2</sub>. Complex **2** is a very rare example of a weakly solvated monomeric cationic form of the [Mn–aryl]<sup>+</sup> functionality, and its chemistry has not yet been explored. We then turned our attention to the ionization of **1** in toluene, to avoid any binding solvent containing donor atoms. Depending on the Mn/BPh<sub>3</sub> ratio and the reaction time, the products reported in reactions 3 (compound **3**) and 4 (compound **4**) were obtained.

(8) Kaminsky, W.; Külper, K.; Brintzinger, H. H.; Wild, F. R. W. P. *Angew. Chem., Int. Ed. Engl.* **1985**, *24*, 507. Ewen, J. A. Haspeslagh, L.; Atwood, J. L.; Zhang, H. *J. Am. Chem. Soc.* **1987**, *109*, 6544. Ewen, J. A.; Jones, R. L.; Razavi, A.; Ferrara, J. D. *J. Am. Chem. Soc.* **1988**, *110*, 6255. Hlatky, G. G.; Turner, H. W.; Eckman, R. R. *J. Am. Chem. Soc.* **1989**, *111*, 2728. Yang, X.; Stern, C. L.; Marks, T. *J. Am. Chem. Soc.* **1991**, *113*, 3623. Collins, S.; Gauthier, W. J.; Holden, D. A.; Kuntz, B. A.; Taylor, N. J.; Ward, D. G. *Organometallics* **1991**, *10*, 2061. Resconi, L.; Piemontesi, F.; Franciscano, L.; Abis, L.; Fiorani, T. *J. Am. Chem. Soc.* **1992**, *114*, 1025. Burger, P.; Diebold, J.; Gutmann, S.; Hund, H. U.; Brintzinger, H. H. *Organometallics* **1992**, *11*, 1319. Marks, T. *Acc. Chem. Res.* **1992**, *25*, 57. Coates, G. W.; Waymouth, R. M. *J. Am. Chem. Soc.* **1993**, *115*, 91. Erker, G.; Aulbach, M.; Knickmeier, M.; Wingbermühle, D.; Krüger, C.; Nolte, M.; Werner, S. *J. Am. Chem. Soc.* **1993**, *115*, 4590. Guerra, G.; Cavallo, L.; Moscardi, G.; Vacatello, M.; Corradini, P. *J. Am. Chem. Soc.* **1994**, *116*, 2988.

(9) Gallo, E.; Solari, E.; De Angelis, S.; Floriani, C.; Re, N.; Chiesi-Villa, A.; Rizzoli, C. *J. Am. Chem. Soc.* **1993**, *115*, 9850.

(10) (a) Brookhart, M.; Grant, B.; Volpe, A. F., Jr. *Organometallics* **1992**, *11*, 3920. (b) Yang, X.; Stern, C. L.; Marks, T. *J. Am. Chem. Soc.* **1994**, *116*, 10015. (c) Pellecchia, C.; Grassi, A.; Zambelli, A. *J. Chem. Soc., Chem. Commun.* **1993**, 947. (d) Pellecchia, C.; Immirzi, A.; Pappalardo, D.; Peluso, A. *Organometallics* **1994**, *13*, 3773. (e) Jia, L.; Yang, X.; Stern, C.; Marks, T. *J. Organometallics* **1994**, *13*, 3755. (f) Quyoum, R.; Wang, Q.; Tudoret, M.-J.; Baird, M. C. *J. Am. Chem. Soc.* **1994**, *116*, 6435. (g) Yang, X.; Stern, C. L.; Marks, T. *J. Angew. Chem., Int. Ed. Engl.* **1992**, *31*, 1375.



Longer reaction times and higher  $\text{BPh}_3/\text{Mn}$  ratios produce exclusively **4**, instead of **3** (see Experimental Section). Both compounds represent masked forms of cationic arylmanganese(II), but with some major differences. In complex **3**, the coordinatively unsaturated metal ion is, to some extent, satisfied by its interaction with  $\text{BPh}_4^-$ . The formation of  $\text{BPh}_4^-$  indicates that a facile mechanism exists for the scrambling (see above) of the aryl groups around boron. In the case of **4**, such scrambling occurs not only between boron-aryl units but also with manganese-aryl units, giving only phenyl groups in its structure. This complex contains a dimeric cationic manganese-phenyl  $[\text{Mn}_2\text{Ph}_2]^{2+}$  fragment weakly complexed by two  $\text{BPh}_4^-$  anions. The occurrence of the  $[\text{Mn}_2\text{Ph}_2]^{2+}$  cation in the dimeric complex **4** rather than  $[\text{Mn}-\text{Mes}]^+$  in the monomeric form **3** may be due to a difference in steric hindrance of the aryl groups, the mesityl preferring to bond in a terminal rather than in a bridging fashion like the phenyl group.

In recent years, a number of cases have been reported in which  $\text{BPh}_4^-$  does not behave as an innocent anion but rather as a protecting group for coordinatively unsaturated transition-metal ions.  $\text{BPh}_4^-$  is capable of displaying different binding modes, going from  $\eta^2$  to  $\eta^6$  binding of a phenyl group to two bent  $\eta^6$ -phenyls surrounding a single metal ion.<sup>11</sup>

A general method for the generation of masked cationic organometallics is by reaction of  $\text{BPh}_3$  with the organometallic to produce, *via* ionization reaction, a weakly binding anion. Nevertheless, the occurrence of ion-pair forms **3** and **4** is rather unique in organometallic chemistry in the absence of an ancillary ligand such as a cyclopentadienyl group. In addition, we should mention that for this purpose we only need a rather weak Lewis acid, instead of the much more powerful  $\text{B}(\text{C}_6\text{F}_5)_3$ .<sup>10</sup>

**Structural Studies in the Solid State.** The high lability of the Mn(II) coordination sphere makes a solid-state/solution-state structural correlation quite difficult, especially in the absence of any spectroscopic solution information. This is particularly true with some polynuclear or ion-pair species such as those dealt with in the present report.

The structure of **1** is given in Figure 1. Selected bond distances and angles are listed in Table 6. The molecule

consists of a linear trimer ( $\text{Mn2}-\text{Mn1}-\text{Mn3} = 178.8(1)^\circ$ ) with four bridging and two terminal mesityl groups. The central Mn1 atom has a distorted-tetrahedral coordination, while the two end Mn2 and Mn3 atoms achieve a trigonal coordination through a terminal mesityl ligand. The deviations from the plane defined by the three carbon atoms are 0.150(1) and 0.177(2) Å for Mn2 and Mn3, respectively. The two four-membered dinuclear rings are planar within experimental errors, the outer metal atoms lying nearly on the plane (*i.e.* Mn3 is 0.047(2) Å from the plane through Mn1, C1, Mn2, and C11; Mn2 is 0.026(2) Å from the plane through Mn1, C21, Mn3, and C31). They form a dihedral angle of  $75.9(3)^\circ$ . The internal C-Mn1-C and Mn-C-Mn angles (mean values  $98.1(3)$  and  $77.9(3)^\circ$ , respectively) result in Mn··Mn distances ( $\text{Mn1}-\text{Mn2} = 2.851(2)$  Å and  $\text{Mn1}-\text{Mn3} = 2.852(2)$  Å) which are longer than those observed in  $[\text{Mn}_2\text{Ph}_6]^{2-5f}$  anions (2.733(1) and 2.763(1) Å). The bridging aromatic rings are nearly perpendicular to the respective  $\text{Mn}_2\text{C}_2$  dimetallacyclobutanes, forming dihedral angles of  $85.2(2)^\circ$  for both  $\text{C1}\cdots\text{C6}$  and  $\text{C11}\cdots\text{C16}$  with respect to the Mn1,Mn2,C1,C11 plane and of  $89.7(2)^\circ$  ( $\text{C21}\cdots\text{C26}$ ) and  $88.2(2)^\circ$  ( $\text{C31}\cdots\text{C36}$ ) with respect to the Mn1,Mn3,C21,C31 plane. The remarkable distortion from tetrahedral coordination around the Mn1 atom (Table 6) is most likely due to the steric hindrance from the bridging mesityl group. The terminal (average 2.122(7) Å) and bridging (average 2.331(5) Å) Mn-C bond distances are close to those in some monomeric, *e.g.*  $[\text{MnMes}_3]^{-5f}$  ( $\text{Mn}-\text{C}_{\text{av}} = 2.141(6)$  Å), and dimeric, *e.g.*  $[\text{Mn}_2\text{Ph}_6]^{2-5f}$  ( $\text{Mn}-\text{C}_{\text{av}} = 2.255(4)$  and 2.285(4) Å), arylmanganese complexes. The coordinative unsaturation of Mn2 and Mn3 is partially completed by some significant Mn··H interactions (Å): Mn2··H91, 2.71; Mn2··H171, 2.90; Mn··H491, 2.95; Mn3··H271, 2.75; Mn3··H391, 2.81; Mn3··H591, 2.94 Å. The Mn2 and Mn3 atoms are displaced remarkably from the terminal mesityl ring plane, the displacements from  $\text{C41}\cdots\text{C46}$  and  $\text{C51}\cdots\text{C56}$  rings being 0.360(1) and 0.646(2) Å for Mn2 and Mn3, respectively. These rings are tilted by  $21.6(3)$  and  $22.5(3)^\circ$  with respect to their coordination planes. All the aromatic rings deviate slightly but significantly from planarity and show the longest C-C bonds at the carbon bonded to Mn. All the methyl groups lie significantly out of their respective aromatic ring planes in a range of 0.05(1)–0.25(1) Å for the bridging mesityls and of 0.03(1)–0.14(1) Å for the terminal ones.

Complex **2** crystallizes as separated monomeric cations  $[\text{Mn}(\text{Mes})(\text{Et}_2\text{O})_3]^+$  and  $\text{BPh}_4^-$  anions. The structure of the cation is given in Figure 2. Selected bond distances and angles are listed in Table 7. The manganese atom displays a distorted-tetrahedral coordination involving a terminal mesityl ligand and three oxygen atoms from diethyl ether molecules. The direction of the Mn-C1 bond is nearly perpendicular to the plane of the oxygen atoms (dihedral angle  $80.1(2)^\circ$ ), from which the Mn protrudes by 1.051(2) Å. The aromatic ring is perpendicular to the oxygen plane, the dihedral angle they form being  $84.6(2)^\circ$ . Distortions from an idealized coordination geometry appear to be related to intraligand steric effects involving the *o*-methyl substituents and the diethyl ethers. Thus, the angles  $\text{O1}-\text{Mn1}-\text{C1}$  ( $121.1(2)^\circ$ ) and  $\text{O2}-\text{Mn1}-\text{C1}$  ( $127.8(3)^\circ$ ) are opened beyond  $109^\circ$ , leading to closure of the O-Mn1-O

(11) (a) Bochmann, M. *Angew. Chem., Int. Ed. Engl.* **1992**, *31*, 1181. (b) Bochmann, M.; Karger, G.; Jaggard, A. J. *J. Chem. Soc., Chem. Commun.* **1990**, 1038. (c) Horton, A. D.; Frijns, J. H. G. *Angew. Chem., Int. Ed. Engl.* **1991**, *30*, 1152. (d) Calderazzo, F.; Englert, U.; Pampaloni, G.; Rocchi, L. *Angew. Chem., Int. Ed. Engl.* **1992**, *31*, 1235. (e) Strauss, S. H. *Chem. Rev.* **1993**, *93*, 927. (f) Pasquali, M.; Floriani, C.; Gaetani-Manfredotti, A. *Inorg. Chem.* **1980**, *19*, 1191.

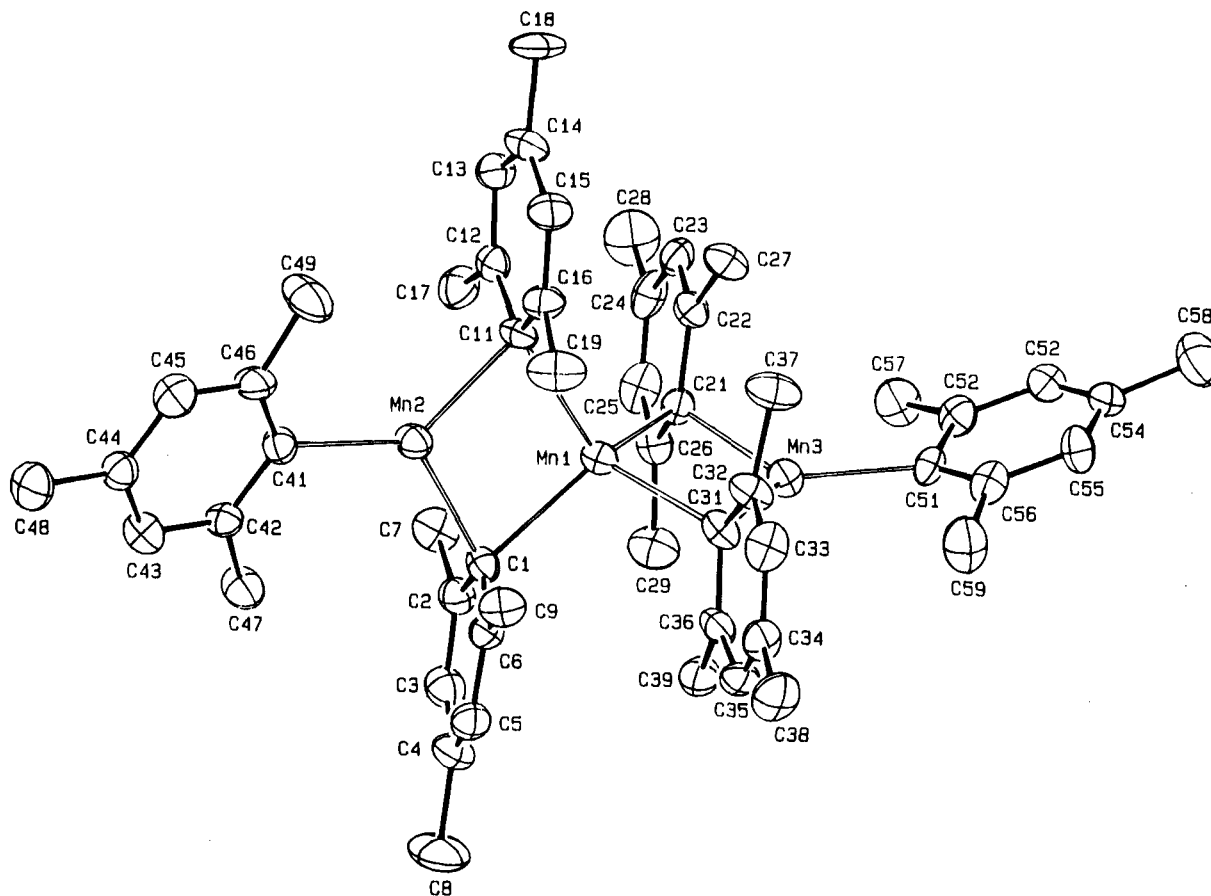


Figure 1. ORTEP drawing for complex 1 (30% probability ellipsoids).

Table 1. Experimental Data for the X-ray Diffraction Studies on Crystalline Compounds 1–4

	1	2	3	4
formula	C <sub>54</sub> H <sub>66</sub> Mn <sub>3</sub> ·C <sub>7</sub> H <sub>8</sub>	C <sub>21</sub> H <sub>41</sub> MnO <sub>3</sub> ·C <sub>24</sub> H <sub>20</sub> B	C <sub>33</sub> H <sub>31</sub> BMn·C <sub>7</sub> H <sub>8</sub>	C <sub>60</sub> H <sub>50</sub> B <sub>2</sub> Mn <sub>2</sub> ·1.5C <sub>7</sub> H <sub>8</sub>
<i>a</i> , Å	12.850(3)	11.237(2)	10.070(1)	15.074(4)
<i>b</i> , Å	20.327(4)	19.035(2)	15.901(1)	13.289(4)
<i>c</i> , Å	11.407(3)	10.991(1)	20.876(2)	28.139(5)
$\alpha$ , deg	95.11(2)	99.30(1)	90	90
$\beta$ , deg	114.00(2)	106.66(1)	101.94(1)	98.39(2)
$\gamma$ , deg	98.77(2)	104.58(1)	90	90
<i>V</i> , Å <sup>3</sup>	2652.2(12)	2109.3(5)	3270.4(5)	5576.4(25)
<i>Z</i>	2	2	4	4
fw	972.1	715.7	585.5	1040.8
space group	<i>P</i> $\bar{1}$ (No. 2)	<i>P</i> $\bar{1}$ (No. 2)	<i>P</i> 2 <sub>1</sub> / <i>n</i> (No. 14)	<i>P</i> 2 <sub>1</sub> / <i>c</i> (No. 14)
<i>t</i> , °C	22	22	22	22
$\lambda$ , Å	0.710 69	1.541 78	1.541 78	1.541 78
$\rho_{\text{calc}}$ , g cm <sup>-3</sup>	1.217	1.127	1.189	1.240
$\mu$ , cm <sup>-1</sup>	7.1	28.1	34.6	40.0
transmissn coeff	0.938–1.000	0.603–1.000	0.547–1.000	0.662–1.000
<i>R</i> <sup>a</sup>	0.052	0.058	0.054 <sup>e</sup>	0.055 <sup>e</sup>
<i>R</i> <sub>w</sub> <sup>b</sup>	0.060	0.070	—	—
wR2 <sup>c</sup>	—	—	0.171 <sup>f</sup>	0.175 <sup>f</sup>
GOF <sup>d</sup>	0.961	1.250	0.820	0.805

<sup>a</sup>  $R = \sum |\Delta F| / \sum |F_o|$ . <sup>b</sup>  $R_w = [\sum w^{1/2} |\Delta F| / \sum w^{1/2} |F_o|]$ . <sup>c</sup>  $wR2 = [\sum (w \Delta F^2) / \sum (w F_o^2)]^{1/2}$ . <sup>d</sup>  $GOF = [\sum w |\Delta F| / (\text{NO} - \text{NV})]^{1/2}$ . <sup>e</sup> For unique observed data. <sup>f</sup> For unique total data.

angles, in particular for the O1–Mn1–O2 angle (89.4(2)°). The Mn–C distance is in agreement with that observed in complex 1 for the terminal Mn–Mes bond. The Mn atom is significantly displaced from the plane of the aromatic ring by 0.088(1) Å.

Structures of 3 and 4 are displayed in Figures 3 and 4, respectively, and the corresponding structural parameters are listed in Tables 8 and 9, respectively. Both compounds contain, in masked form, the cationic functionality [Mn–aryl]<sup>+</sup> as a monomer in 3 and as a dimer in 4, the steric hindrance of the aryl moiety determining

either the monomeric or the dimeric arrangement. The Mn–C(mesityl) distance in 3 is particularly short (2.066(5) Å) compared to those reported for all the other terminal Mn–Mes derivatives, including 1 and 2. An equally short Mn–C distance is observed for the bridging phenyl (Mn–C<sub>av</sub> = 2.197(6) Å) in 4 compared to the other bridging manganese–aryl complexes, including 1 (Mn–C<sub>av</sub> = 2.331(5) Å). The two bridging phenyl rings give rise to a dinuclear four-membered ring which is significantly puckered, the displacements of atoms from the least-squares mean plane being as follows (Å): Mn1,

**Table 2. Fractional Atomic Coordinates ( $\times 10^4$ ) for Complex 1**

atom	<i>x/a</i>	<i>y/b</i>	<i>z/c</i>	atom	<i>x/a</i>	<i>y/b</i>	<i>z/c</i>
Mn1	-14.5(11)	2491.7(6)	2689.3(12)	C33	792(9)	1291(5)	5826(9)
Mn2	-1742.4(11)	1691.6(6)	266.5(13)	C34	1643(9)	983(5)	5732(8)
Mn3	1736.6(11)	3268.1(6)	5026.6(12)	C35	2260(8)	1269(4)	5116(9)
C1	166(7)	1814(4)	1013(7)	C36	2010(8)	1844(4)	4534(8)
C2	728(8)	2167(4)	319(8)	C37	-248(9)	2237(5)	5676(10)
C3	1584(8)	1923(5)	79(9)	C38	1837(10)	320(5)	6236(10)
C4	1903(8)	1315(5)	447(9)	C39	2793(8)	2142(5)	3952(9)
C5	1290(8)	947(4)	1013(9)	C41	-2923(7)	937(4)	-1323(8)
C6	466(8)	1190(4)	1306(8)	C42	-2568(7)	639(4)	-2238(8)
C7	350(9)	2773(5)	-253(9)	C43	-3260(8)	75(4)	-3132(9)
C8	2846(10)	1054(6)	157(13)	C44	-4351(8)	-215(4)	-3216(8)
C9	-158(8)	727(4)	1904(9)	C45	-4715(7)	93(5)	-2389(10)
C11	-2033(7)	2319(4)	1756(8)	C46	-4045(7)	658(5)	-1487(9)
C12	-2547(7)	2852(4)	1165(8)	C47	-1412(8)	926(5)	-2247(9)
C13	-3505(8)	3027(4)	1309(9)	C48	-5091(8)	-839(5)	-4229(10)
C14	-3959(8)	2709(5)	2053(10)	C49	-4572(9)	966(6)	-645(12)
C15	-3501(8)	2172(5)	2596(9)	C51	2732(7)	3857(4)	6905(8)
C16	-2594(8)	1971(4)	2429(9)	C52	2909(7)	4567(5)	7068(8)
C17	-2090(8)	3226(5)	343(9)	C53	3227(8)	4957(5)	8279(9)
C18	-4962(9)	2930(6)	2292(11)	C54	3424(8)	4652(5)	9384(9)
C19	-2259(9)	1324(5)	2884(11)	C55	3296(8)	3970(5)	9213(8)
C21	722(7)	3658(4)	3254(7)	C56	3003(7)	3576(5)	8049(8)
C22	-87(8)	4019(4)	3450(8)	C57	2763(9)	4934(5)	5921(9)
C23	-290(8)	4610(5)	2968(8)	C58	3733(9)	5074(6)	10644(10)
C24	275(9)	4883(5)	2283(9)	C59	2976(10)	2821(5)	7988(9)
C25	1109(9)	4583(5)	2134(9)	C61	5978(9)	3620(4)	6246(8)
C26	1340(8)	3978(4)	2608(8)	C62	5415(9)	3182(4)	6780(8)
C27	-722(9)	3773(4)	4248(9)	C63	5723(9)	2560(4)	7001(8)
C28	46(11)	5524(5)	1734(11)	C64	6593(9)	2376(4)	6689(8)
C29	2364(9)	3718(5)	2538(10)	C65	7156(9)	2814(4)	6155(8)
C31	1131(8)	2170(4)	4594(8)	C66	6849(9)	3436(4)	5934(8)
C32	558(8)	1879(4)	5328(8)	C67	5650(15)	4218(9)	6002(15)

**Table 3. Fractional Atomic Coordinates ( $\times 10^4$ ) for Complex 2<sup>a</sup>**

atom	<i>x/a</i>	<i>y/b</i>	<i>z/c</i>	atom	<i>x/a</i>	<i>y/b</i>	<i>z/c</i>
Mn1	1936.3(11)	2057.3(6)	1145.8(11)	C19B	5448(33)	2237(20)	2041(30)
B1	3767(8)	6826(4)	2325(8)	C20B	3567(27)	3278(13)	3198(28)
O1	2207(4)	1248(2)	-264(5)	C21B	4384(28)	4107(15)	3499(29)
O2	1528(5)	2681(3)	-289(5)	C31	4816(7)	3337(4)	-2755(7)
O3	3885(6)	2704(4)	2316(5)	C32	4750(8)	4049(4)	-2351(9)
C1	835(7)	1718(4)	2335(6)	C33	3604(10)	4242(5)	-2758(10)
C2	-153(7)	2025(4)	2469(7)	C34	2457(9)	3699(6)	-3589(10)
C3	-923(7)	1780(4)	3214(7)	C35	2460(8)	2992(5)	-3984(8)
C4	-743(8)	1228(5)	3858(7)	C36	3628(8)	2813(4)	-3570(7)
C5	254(8)	948(4)	3785(7)	C41	2943(7)	6556(4)	3280(6)
C6	1030(7)	1175(4)	3041(7)	C42	2159(8)	6945(5)	3678(7)
C7	-391(10)	2667(5)	1869(9)	C43	1379(9)	6691(7)	4403(8)
C8	-1595(10)	961(6)	4634(10)	C44	1410(10)	6039(7)	4792(9)
C9	2133(8)	846(5)	3063(8)	C45	2138(10)	5643(5)	4425(10)
C10	2973(9)	1419(5)	-1128(10)	C46	2926(8)	5895(4)	3696(8)
C11	2154(12)	1149(6)	-2562(10)	C51	4011(6)	7732(4)	2420(7)
C12	1507(8)	458(4)	-500(8)	C52	3793(6)	8031(4)	1314(7)
C13	2372(11)	-24(5)	-297(10)	C53	4063(8)	8811(5)	1437(10)
C14	2503(9)	3335(5)	-337(8)	C54	4539(9)	9305(4)	2659(11)
C15	2176(11)	4034(5)	-77(11)	C55	4751(10)	9032(5)	3755(10)
C16	245(9)	2494(5)	-1324(8)	C56	4491(8)	8266(4)	3636(8)
C17	-564(8)	1719(5)	-1448(8)	C61	2873(7)	6343(3)	792(6)
C18A	5098(14)	2615(9)	2088(15)	C62	3441(8)	6302(4)	-186(7)
C19A	5388(16)	1922(8)	2509(16)	C63	2694(11)	5910(5)	-1488(8)
C20A	4189(16)	3052(8)	3713(11)	C64	1375(10)	5566(5)	-1836(8)
C21A	3772(18)	3748(9)	3610(18)	C65	788(8)	5601(4)	-906(8)
C18B	5027(38)	2534(30)	3170(24)	C66	1523(7)	5990(4)	382(7)

<sup>a</sup> The site occupation factors for C18, C19, C20, and C21 are 0.65 and 0.35 for A and B, respectively.

-0.002(1) Å; Mn2, -0.002(1) Å; C81, 0.079(7) Å; C91, 0.085(7) Å. The internal C-Mn-C and Mn-C-Mn angles (mean values 100.9(3) and 79.0(3)°, respectively) result in a Mn···Mn distance of 2.796(1) Å. The C81···C86 and C91···C96 bridging rings form dihedral angles of 91.6(2) and 107.2(2)° with the Mn<sub>2</sub>C<sub>2</sub> core indicating some structural distortions.

The very important, novel feature of the structures of **3** and **4** is the interaction between Mn and the BPh<sub>4</sub><sup>-</sup> anions, acting in both cases as a bent-sandwich ligand.

In both cases, we observe rather long Mn-C(BPh<sub>4</sub><sup>-</sup>) distances, implying rather weak interactions, as expected for the kind of ion pairing held by electrostatic interactions. The interaction modes are, however, significantly different in **3** and **4**. Although varying over a large range (see Table 8), the Mn-C(BPh<sub>4</sub><sup>-</sup>) distances in complex **3** suggest a  $\eta^3$  bonding to the C11···C16 and C21···C26 phenyl rings. The manganese experiences a kind of bent bis(allyl) binding. The C11,C12,C16 centroid and the C21,C22,C26 centroid to Mn distances

**Table 4. Fractional Atomic Coordinates ( $\times 10^4$ ) for Complex 3**

atom	<i>x/a</i>	<i>y/b</i>	<i>z/c</i>	atom	<i>x/a</i>	<i>y/b</i>	<i>z/c</i>
Mn1	428.2(8)	1646.6(5)	2844.1(4)	C32	1415(6)	4684(3)	3457(2)
B1	51(5)	3567(3)	2636(3)	C33	1567(7)	5284(4)	3943(3)
C1	540(4)	427(3)	3193(3)	C34	440(9)	5475(4)	4217(3)
C2	246(4)	-270(3)	2768(3)	C35	-761(8)	5073(4)	3995(3)
C3	243(5)	-1078(4)	3023(4)	C36	-879(6)	4482(3)	3508(2)
C4	496(5)	-1228(4)	3686(4)	C41	-314(4)	4096(3)	1952(2)
C5	822(5)	-544(4)	4101(3)	C42	678(5)	4421(3)	1645(2)
C6	819(5)	268(3)	3867(2)	C43	366(6)	4900(3)	1084(2)
C7	-82(6)	-160(4)	2027(2)	C44	-963(6)	5083(3)	800(2)
C8	403(7)	-2100(4)	3951(4)	C45	-1973(5)	4783(3)	1096(2)
C9	1142(6)	981(4)	4350(3)	C46	-1640(5)	4292(3)	1658(2)
C11	1422(4)	2978(3)	2687(2)	C51A	5502(9)	3160(5)	4848(6)
C12	1633(5)	2525(3)	2130(3)	C52A	5369(14)	2405(7)	5169(7)
C13	2622(6)	1923(4)	2178(3)	C53A	4135(13)	2272(8)	5357(7)
C14	3477(6)	1734(4)	2767(4)	C54A	3084(15)	2856(7)	5301(8)
C15	3311(6)	2165(4)	3318(3)	C55A	3288(10)	3661(8)	5073(7)
C16	2302(5)	2772(3)	3274(2)	C56	4455(7)	3743(4)	4817(4)
C21	-1105(4)	2840(3)	2684(2)	C57A	6679(14)	3389(10)	4513(8)
C22	-1384(5)	2544(3)	3282(3)	C51B	3913(9)	3048(5)	5081(5)
C23	-2227(7)	1866(4)	3318(4)	C52B	4682(12)	2326(7)	5267(7)
C24	-2824(6)	1452(4)	2748(4)	C53B	6003(13)	2237(8)	5169(7)
C25	-2570(5)	1706(3)	2156(4)	C54B	6524(13)	2878(7)	4837(7)
C26	-1728(5)	2378(3)	2134(3)	C55B	5748(9)	3607(7)	4694(7)
C31	215(5)	4250(3)	3229(2)	C57B	2446(11)	3133(11)	5181(9)

<sup>a</sup> The site occupation factor is 0.5 for the A and B positions of C51, C52, C53, C54, C55, and C57.

**Table 5. Fractional Atomic Coordinates ( $\times 10^4$ ) for Complex 4<sup>a</sup>**

atom	<i>x/a</i>	<i>y/b</i>	<i>z/c</i>	atom	<i>x/a</i>	<i>y/b</i>	<i>z/c</i>
Mn1	1605.9(6)	-859.8(7)	1888.8(3)	C61	-1119(3)	-919(4)	1776(2)
Mn2	3169.3(6)	-772.0(7)	2558.1(4)	C62	-902(4)	-711(4)	2263(2)
B1	4499(4)	-588(5)	3442(2)	C63	-1518(4)	-802(4)	2582(2)
B2	-361(4)	-861(5)	1406(2)	C64	-2376(5)	-1104(5)	2428(3)
C1	4514(3)	-8(4)	2921(2)	C65	-2627(4)	-1306(5)	1950(3)
C2	5014(4)	-414(5)	2577(2)	C66	-1999(4)	-1211(4)	1628(2)
C3	5066(4)	42(6)	2134(2)	C71	-860(4)	-903(5)	853(2)
C4	4613(5)	939(6)	2024(3)	C72	-1182(4)	-1802(5)	638(3)
C5	4110(5)	1349(5)	2342(3)	C73	-1682(5)	-1820(7)	193(3)
C6	4063(4)	895(5)	2777(2)	C74	-1866(7)	-976(10)	-57(3)
C11	3770(3)	-1550(4)	3376(2)	C75	-1568(7)	-64(8)	133(4)
C12	3764(4)	-2259(4)	3017(2)	C76	-1073(5)	-42(6)	579(3)
C13	3240(4)	-3115(5)	2984(3)	C81	1793(3)	-300(5)	2625(2)
C14	2689(4)	-3297(5)	3322(3)	C82	1429(4)	-874(5)	2971(2)
C15	2681(4)	-2625(6)	3692(3)	C83	1003(4)	-445(6)	3315(3)
C16	3195(4)	-1772(5)	3721(2)	C84	923(4)	587(7)	3327(3)
C21	4218(4)	204(4)	3848(2)	C85	1272(4)	1183(5)	3009(3)
C22	4790(4)	474(5)	4255(2)	C86	1705(4)	746(5)	2670(2)
C23	4549(5)	1137(5)	4597(3)	C91	2999(4)	-1220(5)	1796(3)
C24	3708(6)	1554(5)	4527(3)	C92	3229(5)	-581(6)	1407(4)
C25	3123(5)	1311(5)	4132(3)	C93	3753(6)	-855(8)	1062(3)
C26	3363(4)	632(5)	3802(2)	C94	4129(7)	-1771(9)	1073(4)
C31	5495(4)	-1056(4)	3632(2)	C95	3973(6)	-2446(7)	1434(4)
C32	5615(4)	-1942(4)	3903(2)	C96	3427(5)	-2154(6)	1755(3)
C33	6448(4)	-2267(5)	4115(2)	C1SA	8115(10)	1163(11)	5144(5)
C34	7199(4)	-1713(5)	4070(2)	C1SB	9066(17)	1167(16)	5318(9)
C35	7110(4)	-849(5)	3807(2)	C2S	8523(8)	299(8)	5262(4)
C36	6282(4)	-525(4)	3592(2)	C3SA	9435(13)	205(15)	5452(7)
C41	358(4)	-1814(4)	1506(2)	C3SB	7570(17)	556(18)	5021(8)
C42	555(3)	-2298(4)	1944(2)	C4S	9952(10)	1183(12)	5506(5)
C43	1146(4)	-3111(4)	2023(2)	C5SA	9575(13)	2000(13)	5371(6)
C44	1545(4)	-3470(5)	1652(3)	C5SB	7947(16)	2231(16)	5007(8)
C45	1380(5)	-3023(5)	1210(3)	C6S	8734(9)	2100(9)	5199(4)
C46	804(4)	-2208(5)	1135(2)	C7S	7210(9)	1373(11)	4936(5)
C51	204(4)	210(4)	1487(2)	C8S	4782(7)	889(7)	0(4)
C52	991(4)	366(4)	1282(2)	C9S	5498(15)	1055(16)	349(8)
C53	1453(4)	1282(5)	1320(2)	C10S	6034(9)	320(12)	565(5)
C54	1142(4)	2062(5)	1554(2)	C11S	5869(12)	-669(15)	339(7)
C55	364(4)	1951(4)	1758(2)	C12S	4601(14)	-107(19)	-203(8)
C56	-83(4)	1049(4)	1723(2)				

<sup>a</sup> The site occupation factor is 0.5 for C1SA, C1SB, C3SA, C3SB, C5SA, C5SB, C9S, C11S, and C12S.

are 2.294(5) and 2.347(5) Å, respectively, while the centroid-Mn-centroid angle is 88.1(2)° and the dihedral angle between the corresponding phenyl rings is 84.7(1)°.

In the case of complex 4, for both Mn1 and Mn2 the

bonding mode of the two adjacent phenyl rings to the metal is  $\eta^2$  (see Table 9) and occurs at rather long distances (from 2.362(5) to 2.659 Å) by rather weak interactions. There are a number of recent and significant examples in which  $\text{BPh}_4^-$  acts as a ligand.<sup>11</sup>

**Table 6. Selected Interatomic Distances (Å) and Angles (deg) for Complex 1**

Mn1-Mn2	2.851(2)	Mn3-C31	2.189(8)
Mn1-Mn3	2.852(2)	Mn3-C51	2.123(7)
Mn1-C1	2.321(9)	C1-C2	1.439(14)
Mn1-C11	2.324(8)	C1-C6	1.410(12)
Mn1-C21	2.343(8)	C11-C12	1.432(12)
Mn1-C31	2.334(8)	C11-C16	1.414(15)
Mn2-C1	2.209(9)	C21-C22	1.436(15)
Mn2-C11	2.220(10)	C21-C26	1.414(14)
Mn2-C41	2.121(7)	C31-C32	1.432(15)
Mn3-C21	2.207(8)	C31-C36	1.415(15)
C21-Mn1-C31	97.8(3)	Mn2-C11-C16	116.6(6)
C11-Mn1-C31	124.2(3)	Mn2-C11-C12	107.2(6)
C11-Mn1-C21	107.6(3)	Mn1-C11-C16	117.2(6)
C1-Mn1-C31	106.0(3)	Mn1-C11-C12	116.8(6)
C1-Mn1-C21	124.8(3)	C12-C11-C16	115.4(8)
C1-Mn1-C11	98.8(3)	Mn1-C21-Mn3	77.6(3)
Mn2-Mn1-Mn3	178.8(1)	Mn3-C21-C26	117.4(6)
C11-Mn2-C41	130.4(4)	Mn3-C21-C22	111.0(5)
C1-Mn2-C41	122.6(3)	Mn1-C21-C26	118.2(6)
C1-Mn2-C11	105.5(3)	Mn1-C21-C22	112.7(6)
C31-Mn3-C51	126.0(3)	C22-C21-C26	114.7(8)
C21-Mn3-C51	125.4(3)	Mn3-C31-C36	110.8(6)
C21-Mn3-C31	106.5(3)	Mn3-C31-C32	116.9(6)
Mn1-C1-Mn2	78.0(3)	Mn1-C31-C36	114.1(6)
Mn2-C1-C6	108.6(6)	Mn1-C31-C32	117.9(7)
Mn2-C1-C2	117.8(6)	C32-C31-C36	114.1(8)
Mn1-C1-C6	116.0(5)	Mn2-C41-C46	123.5(6)
Mn1-C1-C2	115.1(5)	Mn2-C41-C42	120.9(7)
C2-C1-C6	115.8(8)	Mn3-C51-C56	122.3(6)
Mn1-C11-Mn2	77.7(3)	Mn3-C51-C52	120.2(6)

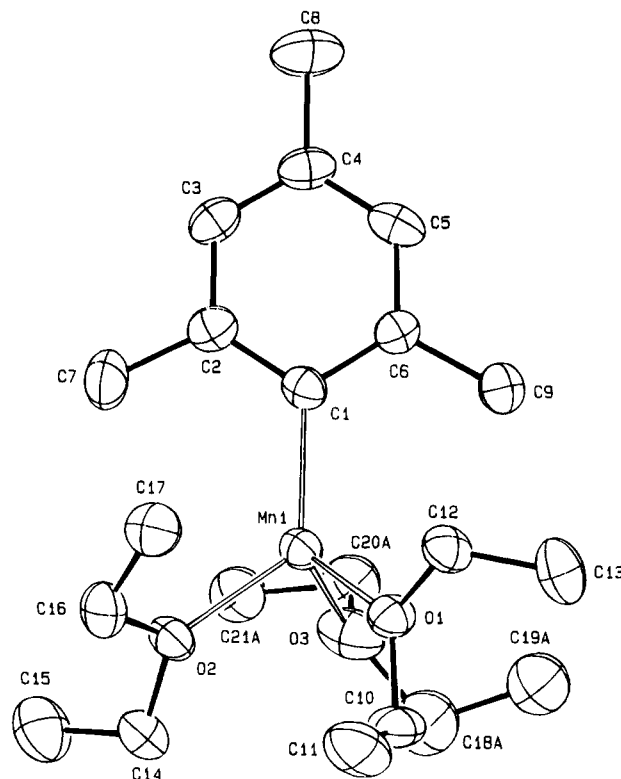
**Table 7. Selected Bond Distances (Å) and Angles (deg) for Complex 2**

Mn1-O1	2.145(5)	O2-C16	1.473(9)
Mn1-O2	2.138(6)	O3-C18A	1.499(19)
Mn1-O3	2.117(5)	O3-C20A	1.473(13)
Mn1-C1	2.111(8)	O3-C18B	1.500(45)
O1-C10	1.475(13)	O3-C20B	1.521(32)
O1-C12	1.452(8)	C1-C2	1.410(12)
O2-C14	1.456(11)	C1-C6	1.412(11)
O3-Mn1-C1	110.6(2)	C14-O2-C16	113.4(6)
O2-Mn1-C1	127.8(3)	Mn1-O3-C20B	97.5(13)
O2-Mn1-O3	100.9(3)	Mn1-O3-C18B	134.3(22)
O1-Mn1-C1	121.1(2)	Mn1-O3-C20A	119.5(8)
O1-Mn1-O3	102.4(2)	Mn1-O3-C18A	126.0(7)
O1-Mn1-O2	89.4(2)	C18B-O3-C20B	106.8(16)
Mn1-O1-C12	119.2(4)	C18A-O3-C20A	109.9(9)
Mn1-O1-C10	125.8(4)	Mn1-C1-C6	122.8(6)
C10-O1-C12	114.8(6)	Mn1-C1-C2	121.4(5)
Mn1-O2-C16	123.7(5)	C2-C1-C6	115.7(7)
Mn1-O2-C14	122.9(5)		

Included among these are the stabilization of the  $[\text{Zr}(\text{CH}_2\text{Ph})_3]^+$  cation<sup>11b</sup> by a  $\eta^6$  interaction of one of the phenyl rings from  $\text{BPh}_4^-$ , the complex  $[\{\text{Ph}_2\text{B}(\eta^6\text{-Ph})_2\}\text{Nb}(\eta^2\text{-C}_2\text{Me}_2)]^{11d}$  containing a  $\text{BPh}_4^-$  ligand acting as a 12-electron donor and behaving as a bent bis( $\eta^6$ -arene) ligand, and the  $\eta^2$ -bonding mode in some cationic indenyl zirconium complexes<sup>11c</sup> and in copper(I) complexes.<sup>11f</sup>

In spite of the fact that the structural parameters seem to indicate a rather weak interaction in such ion-pair forms, the  $\text{BPh}_4^-$  cannot be displaced by electron-rich neutral arenes, an indication of the importance of electrostatic interactions within complexes of this kind.<sup>11a</sup>

**Magnetic Properties.** The magnetic properties of organometallics is a poorly studied field, because a relationship has not been found between the magnetic properties and the chemical behavior, *i.e.* how much the chemistry of the  $[\text{M}-\text{R}]$  fragment depends on the magnetic properties of the metal. On the other hand, the magnetic properties could give vital information on

**Figure 2.** ORTEP drawing for complex 2 (30% probability ellipsoids). For clarity only the A position is given for the disordered C18-C21 carbon atoms.

the nature of alkyl-metal or aryl-metal aggregates, an area of increasing interest both for chemical reactivity and for precursors of solid-state materials.<sup>12</sup> Magnetic studies can also be diagnostic in some cases for the existence of metal-metal bonds.<sup>13</sup> In the present report we deal with a homogeneous class of manganese(II) aryls possessing monomeric, dimeric, and trimeric examples, with the last having a rather short  $\text{Mn} \cdots \text{Mn}$  distance.

Magnetic susceptibility data for complexes 1, 3, and 4 were collected in the temperature range 1.9–300 K, and those for 4 and 1 are displayed in Figures 5 and 6, respectively.

For complex 3 the magnetic moment per manganese ion is essentially constant down to about 60 K with a value of  $5.79 \mu_B$ , which falls in the typical range for Mn(II) complexes,<sup>14,15</sup> and then shows a slight reduction due to a small zero-field splitting.

The susceptibility data for the dimer complex 4 were fitted with the simple theoretical equation<sup>16</sup>

$$\chi_{\text{dim}} = \frac{Ng^2\mu_B^2}{kT} \frac{2e^{2x} + 10e^{6x} + 28e^{12x} + 60e^{20x} + 110e^{30x}}{1 + 3e^{2x} + 5e^{6x} + 7e^{12x} + 9e^{20x} + 11e^{30x}}$$

where  $x = J/kT$ , obtained assuming that the interaction

(12) Trogler, W. C. *Organometallic Radical Processes*; Elsevier: Amsterdam, The Netherlands, 1990.

(13) Klose, A.; Solari, E.; Floriani, C.; Chiesi-Villa, A.; Rizzoli, C.; Re, N. *J. Am. Chem. Soc.* **1994**, *116*, 9123.

(14) Carlin, R. L. *Magnetochemistry*; Springer-Verlag: Berlin, 1986.

(15) Casey, A. T.; Mitra, S. In *Theory and Applications of Molecular Paramagnetism*, Bodreaux, E. A., Mulay, L. N., Eds.; Wiley: New York, 1976, p 135.

(16) O'Connor, C. J. *Prog. Inorg. Chem.* **1982**, *29*, 203.

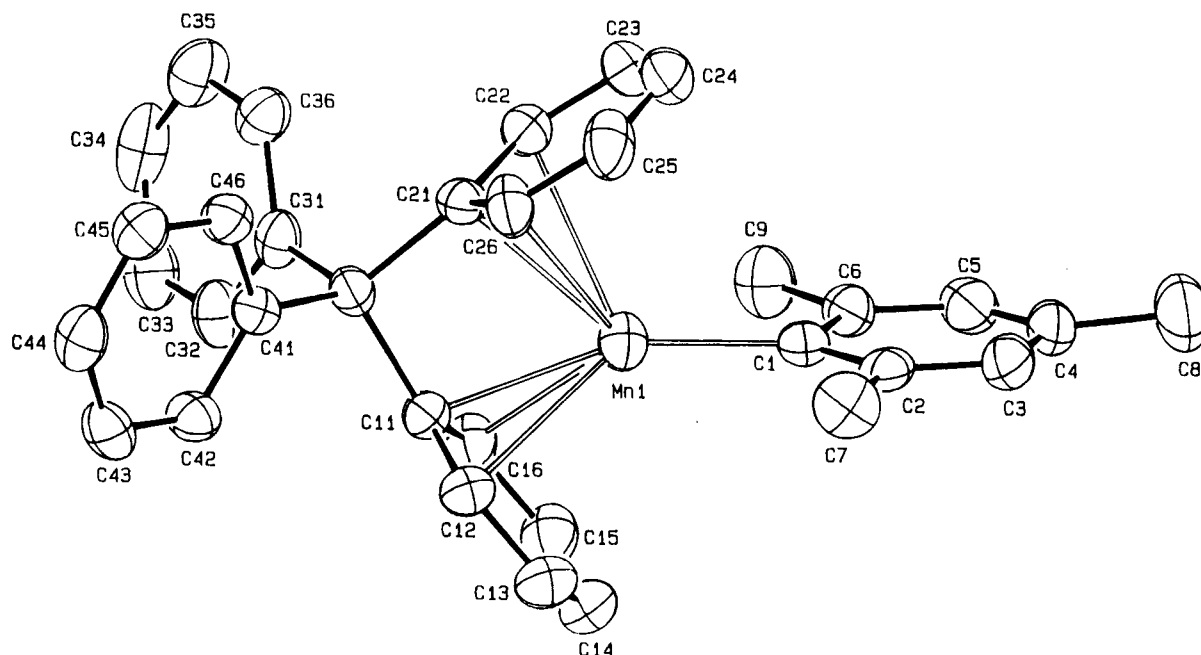


**Figure 3.** ORTEP drawing for complex 3 (30% probability ellipsoids).

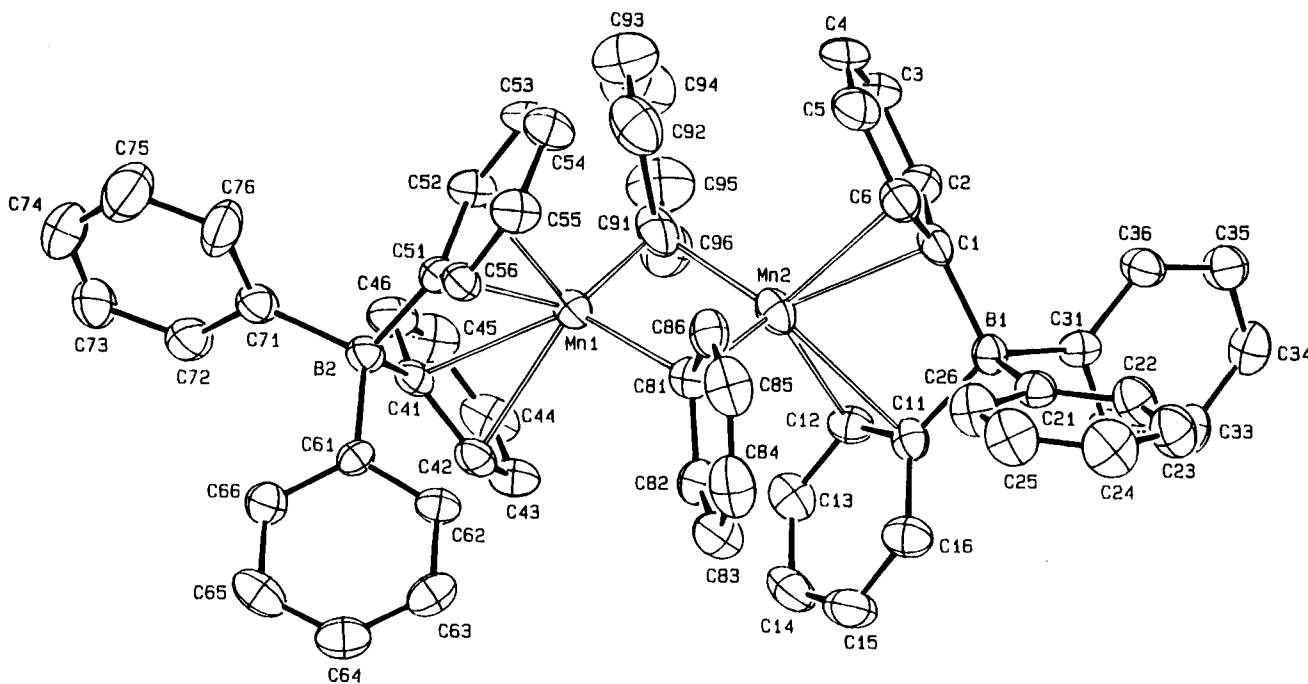


**Figure 4.** ORTEP drawing for complex 4 (30% probability ellipsoids).

between the two spin centers were described by the Heisenberg spin Hamiltonian  $H_{\text{ex}} = -2J\hat{S}_1\cdot\hat{S}_2$ , with  $\hat{S}_1 = \hat{S}_2 = 5/2$ .

The presence of a small Curie tail in the magnetic susceptibility data at low temperature for two of our complexes requires a correction for a small quantity of monomeric Mn(II) impurities which were assumed to obey Curie law. The following equation is therefore obtained for the total susceptibility:

$$\chi = \frac{1}{2}(1-p)\chi_{\text{dim}} + p\frac{Ng'^2\mu_B^2S(S+1)}{3kT} \quad (1)$$

where  $S$  and  $g'$  are the spin and the  $g$  factors of the

impurity (assumed to be the same as for the Mn(II) ion in the dimer) and  $p$  is the monomeric impurity fraction. A good fit ( $R = 9 \times 10^{-4}$ ) to the collected data was obtained for  $g = 1.98$ ,  $J = -55.4 \text{ cm}^{-1}$ , and  $p = 1.8\%$  (see Figure 5).

The situation is more complicated for the trimeric complex 1, for which the temperature dependence of  $\mu_{\text{eff}}$  shows a plateau at about  $3.4 \mu_B$  below 100 K and a very limited increase above that temperature ( $3.65 \mu_B$  at 310 K). These values are much smaller than that expected for three uncoupled Mn(II) ions ( $5.92 \mu_B$ ). This behavior clearly indicates a strong antiferromagnetic coupling between the three Mn(II) centers, with spin frustration, leading to an overall  $S = 5/2$  ground state. Only at very low temperatures, less than 4 K, does  $\mu_{\text{eff}}$  show a very

**Table 8. Selected Interatomic Distances (Å) and Angles (deg) for Complex 3**

Mn1-C1	2.066(5)	Mn1-C23	3.057(8)
Mn1-C11	2.393(5)	Mn1-C24	3.254(6)
Mn1-C12	2.528(6)	Mn1-C25	3.065(5)
Mn1-C13	2.877(7)	Mn1-C26	2.633(5)
Mn1-C14	3.110(7)	C1-C2	1.412(7)
Mn1-C15	2.983(6)	C1-C6	1.400(7)
Mn1-C16	2.621(5)	C11-C12	1.421(8)
Mn1-C21	2.425(5)	C11-C16	1.395(6)
Mn1-C22	2.625(6)	C21-C22	1.416(8)
C21-C26	1.398(7)		
C21-Mn1-C26	31.7(1)	Mn1-C1-C2	121.7(4)
C21-Mn1-C22	32.2(1)	C2-C1-C6	117.5(4)
C11-Mn1-C21	64.0(1)	Mn1-C11-B1	98.2(3)
C11-Mn1-C16	31.9(1)	Mn1-C11-C16	83.1(3)
C11-Mn1-C12	33.4(1)	Mn1-C11-C12	78.5(3)
C1-Mn1-C21	140.3(2)	Mn1-C21-B1	96.8(3)
C1-Mn1-C11	152.2(2)	Mn1-C21-C26	82.3(3)
Mn1-C1-C6	120.6(3)	Mn1-C21-C22	81.7(3)

**Table 9. Selected Interatomic Distances (Å) and Angles (deg) for Complex 4**

Mn1-Mn2	2.796(1)	Mn2-C13	3.332(7)
Mn1-C41	2.391(6)	Mn2-C14	4.106(7)
Mn1-C42	2.502(5)	Mn2-C15	4.180(8)
Mn1-C43	3.106(6)	Mn2-C16	3.527(6)
Mn1-C44	3.531(7)	Mn2-C81	2.202(5)
Mn1-C45	3.441(7)	Mn2-C91	2.204(8)
Mn1-C46	2.902(6)	C1-C2	1.417(8)
Mn1-C51	2.659(6)	C1-C6	1.409(8)
Mn1-C52	2.443(5)	C11-C12	1.380(8)
Mn1-C53	3.257(7)	C11-C16	1.423(8)
Mn1-C54	4.032(7)	C21-C22	1.377(8)
Mn1-C55	4.170(6)	C21-C26	1.397(9)
Mn1-C56	3.576(6)	C31-C32	1.400(8)
Mn1-C81	2.180(6)	C31-C36	1.399(8)
Mn1-C91	2.206(7)	C41-C42	1.383(8)
Mn2-C1	2.362(5)	C41-C46	1.421(9)
Mn2-C2	2.814(6)	C51-C52	1.408(9)
Mn2-C3	3.430(7)	C51-C56	1.398(8)
Mn2-C4	3.622(8)	C81-C82	1.409(9)
Mn2-C5	3.252(7)	C81-C86	1.404(9)
Mn2-C6	2.619(7)	C91-C92	1.466(13)
Mn2-C11	2.565(5)	C91-C96	1.411(10)
Mn2-C12	2.457(5)		
C81-Mn1-C91	101.1(2)	Mn1-C41-B2	97.0(3)
C52-Mn1-C91	109.4(2)	Mn1-C41-C46	95.8(4)
C52-Mn1-C81	114.8(2)	Mn1-C41-C42	78.0(3)
C41-Mn1-C91	122.1(2)	C42-C41-C46	114.8(5)
C41-Mn1-C81	126.4(2)	Mn2-C42-C41	69.2(3)
C41-Mn1-C42	32.7(2)	Mn2-C42-C43	101.9(4)
C51-Mn1-C52	31.7(2)	C41-C42-C43	123.4(5)
C81-Mn2-C91	100.5(3)	Mn1-C51-B2	87.7(3)
C12-Mn2-C91	106.0(2)	Mn1-C51-C56	129.4(4)
C12-Mn2-C81	117.4(2)	Mn1-C51-C52	65.7(3)
C1-Mn2-C91	120.5(2)	C52-C51-C56	114.5(5)
C1-Mn2-C81	126.9(2)	Mn1-C52-C51	82.6(3)
C1-Mn2-C6	32.3(2)	C51-C52-C53	122.5(5)
C11-Mn2-C12	31.8(2)	Mn1-C52-C53	113.1(4)
Mn2-C1-B1	93.5(3)	C62-C61-C66	115.4(5)
Mn2-C1-C6	83.9(3)	C72-C71-C76	115.3(6)
Mn2-C1-C2	92.8(3)	Mn1-C81-Mn2	79.3(2)
C2-C1-C6	114.2(5)	Mn2-C81-C86	113.1(4)
Mn2-C11-B1	86.1(3)	Mn2-C81-C82	111.8(4)
Mn2-C11-C16	121.7(4)	Mn1-C81-C86	115.0(4)
Mn2-C11-C12	69.8(3)	Mn1-C81-C82	117.5(4)
C12-C11-C16	114.7(5)	C82-C81-C86	115.0(5)
Mn2-C12-C11	78.4(3)	Mn1-C91-Mn2	78.7(2)
C11-C12-C13	123.7(6)	Mn2-C91-C96	109.1(6)
Mn2-C12-C13	117.8(4)	Mn2-C91-C92	124.3(5)
C22-C21-C26	115.3(5)	Mn1-C91-C96	130.9(5)
C32-C31-C36	115.1(5)	Mn1-C91-C92	107.2(5)

small decrease, indicating an almost negligible zero-field splitting effect. These data were fitted using the theoretical equation corresponding to the spin Hamil-

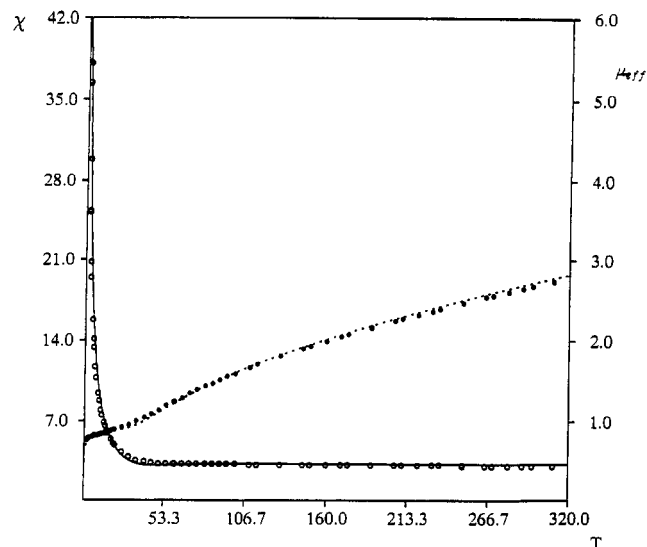


**Figure 5.** Magnetic susceptibility ( $\circ$ ;  $10^{-3} \text{ cm}^3 \text{ mol}^{-1}$ ) and effective magnetic moment ( $\bullet$ ;  $\mu_B$ ) per Mn for **4** as a function of the temperature. The solid and dashed lines are the best theoretical fits (see text) to the experimental data.

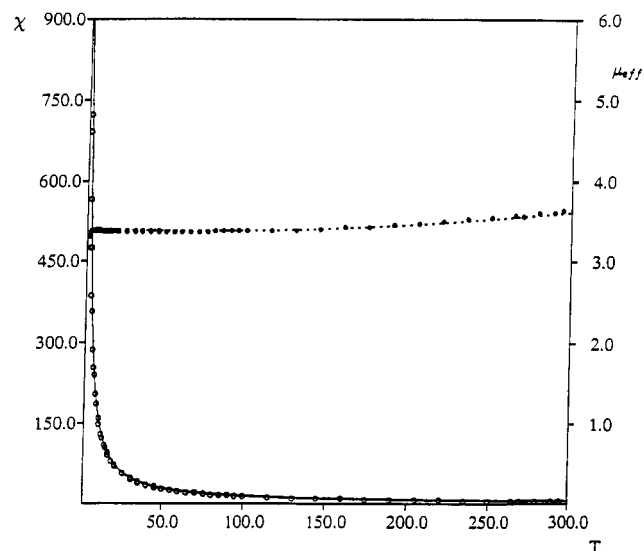


**Figure 6.** Magnetic susceptibility ( $\circ$ ;  $10^{-3} \text{ cm}^3 \text{ mol}^{-1}$ ) and effective magnetic moment ( $\bullet$ ;  $\mu_B$ ) per Mn for **1** as a function of the temperature. The solid and dashed lines are the best theoretical fits (see text) to the experimental data.

tonian

$$\hat{H} = -2J(\hat{S}_1 \cdot \hat{S}_2 + \hat{S}_1 \cdot \hat{S}_3) + g\mu_B H \cdot \hat{S} \quad (2)$$

where  $\hat{S}_1$  is the spin of the central ion,  $\hat{S}_2$  and  $\hat{S}_3$  are the spins of the terminal ions, all being  $5/2$ , and  $\hat{S}$  is the total spin. In this Hamiltonian we assumed equivalent  $g$  factors for the three ions and neglected the coupling between the two terminal ions, both approximations being quite reasonable on the basis of the structure. The spin energy levels may be calculated by Kambe methods,<sup>17</sup> which gives

$$E(S', S) = -J[S(S+1) - S'(S'+1) - s(s+1)] \quad (3)$$

in which  $s = 5/2$  and  $S'$  is the quantum number

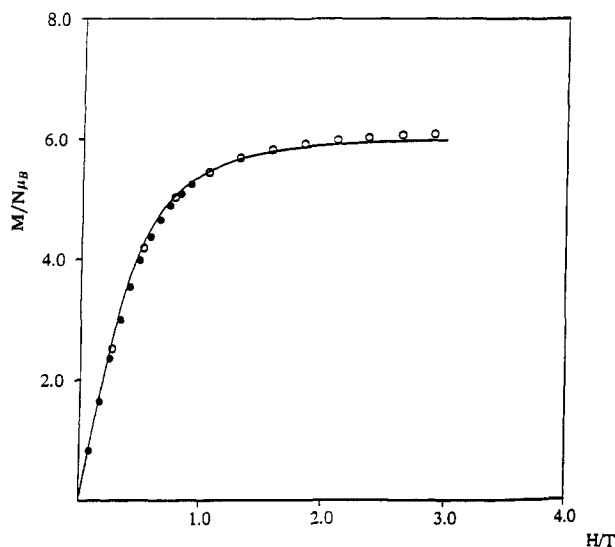


**Figure 7.** Reduced magnetization,  $M/N\mu_B$ , for **4** as a function of  $H/T$  ( $10^{-4}$  G  $K^{-1}$ ) collected at two temperatures: (○) 1.9 K; (●) 6 K. The solid line is the best theoretical fit (see text) to the experimental data.

corresponding to  $\hat{S}' = \hat{S}_2 + \hat{S}_3$ .  $S'$  and  $S$  must satisfy the conditions  $0 \leq S' \leq 5$ ,  $|S' - 5/2| \leq S \leq S' + 5/2$ . We use the expression obtained by inserting these energy levels into the van Vleck equation<sup>18</sup>

$$\chi = \frac{Ng^2\mu_B^2 \sum_S \sum_{S'} S(S+1)(2S+1) \exp[-E(S,S')/kT]}{3kT \sum_S \sum_{S'} (2S+1) \exp[-E(S,S')/kT]}$$

to fit the temperature dependence of  $\chi$  and  $\mu_{\text{eff}}$ . A good fit,  $R = 5 \times 10^{-4}$ , was obtained for  $g = 1.99$  and  $J = -40.4 \text{ cm}^{-1}$  and is shown in Figure 6.

In terms of an energy level scheme, the results above indicate that the  $S = 5/2$  ground state is fairly isolated, with the next excited levels ( $S = 3/2$  at  $101 \text{ cm}^{-1}$  and  $S = 7/2$  at  $141.4 \text{ cm}^{-1}$ ) being high enough in energy to be negligibly populated below 60 K. On the other hand, these energy levels become slightly populated above 100 K, giving rise to a small increase in  $\mu_{\text{eff}}$ . This energy level pattern has been confirmed by isothermal variable-field magnetization measurements taken at 1.9 and 6.0 K. The data are shown in Figure 7 and can both be fitted well with the expression

$$M = Ngm_B SB_{5/2}(z)$$

where  $z = gm_B H/kT$  and  $B_{5/2}(z)$  is the Brillouin function for a  $S = 5/2$  state.<sup>14</sup> In particular, the good fit for the 6 K data clearly indicates that excited energy levels are not populated at that temperature and confirms that they are high in energy.

Complexes **1** and **4** have unique trinuclear and binuclear cores in which dimanganese(II) units held by bridging aryl groups exhibit unusually large negative  $J$  values. Indeed, the coupling constant values found for complexes **1** and **4** show a strong antiferromagnetic coupling for these  $(\mu_2\text{-Ar})_2\text{Mn}^{\text{II}}$  species. It is worth

noting that these values are higher than those usually found for  $\mu$ -alkoxo and  $\mu$ -carboxylato  $\text{Mn}^{\text{II}}\text{-Mn}^{\text{II}}$  dimers<sup>19–22</sup> intensively studied within the investigation of inorganic model complexes of manganese-containing metalloproteins.<sup>22</sup> This strong interaction could be due either to a shorter Mn–Mn distance (2.8–2.9 Å) observed in compounds **1** and **4** versus the longer distances (3.3–4.3) usually observed in the  $\mu$ -alkoxo and  $\mu$ -carboxylato complex or to the higher efficiency for electron exchange of the aromatic carbon bridge. The only previously magnetically characterized manganese trimer containing unsaturated carbon bridges is tetrakis(3-methylpentadienyl)trimanganese.<sup>23</sup> However, it cannot be directly related to complex **1**, as its magnetic behavior has been interpreted in terms of a high-spin (ionic) central  $\text{Mn}^{2+}$  and two low-spin diamagnetic Mn(I) units.<sup>1</sup> A few aryl-bridged manganese(II) complexes are known,<sup>5f</sup> but these have not been magnetically well characterized. The only available value is the magnetic moment at room temperature of  $[\text{Ph}_2\text{Mn}(\mu\text{-Ph})_2\text{MnPh}_2]$ , which at 2.3 BM indicates a considerable antiferromagnetic metal–metal coupling. To date only two other examples of magnetically characterized, mesityl-bridged, dimetal units are known to us:  $[(\text{Mes})\text{Fe}(\mu\text{-Mes})_2\text{Fe}(\text{Mes})]$ ,<sup>13</sup> with  $J = -31.5 \text{ cm}^{-1}$ , and  $[(\text{Mes})\text{Co}(\mu\text{-Mes})_2\text{Co}(\text{Mes})]$ ,<sup>24</sup> where  $J$  is on the order of  $-500 \text{ cm}^{-1}$ . In the latter case the first triplet excited state is thermally inaccessible but is low enough to give rise to a relevant temperature-independent paramagnetism.

The difference between the  $J$  values obtained for the dimer **4** ( $55.4 \text{ cm}^{-1}$ ) and the trimer **1** ( $40.4 \text{ cm}^{-1}$ ) reveals that the coupling constant due to these  $\mu$ -aryl bridges is very sensitive to the metal–metal bond distance (2.851(2) and 2.796(1) Å, respectively, for **1** and **4**). The weaker interaction in complex **1** could be related equally to the larger Mn–Mn distance or to the larger Mn–C–Mn bond angle.

## Experimental Section

**General Procedure.** All operations were carried out under an atmosphere of purified nitrogen using modified Schlenk techniques or in a Braun drybox. Solvents were dried and distilled before use by standard methods. The synthesis of  $\text{BPh}_3$  was carried out as reported in the literature.<sup>25</sup>

**Synthesis of 1.** The Grignard reagent  $\text{MesMgBr}$  (380 mL, 0.334 mmol) was added to a THF (50 mL) solution of  $\text{MnCl}_2 \cdot 1.5\text{THF}$  (37.2 g, 0.159 mmol) cooled to  $-30^\circ\text{C}$ . The brown suspension was then warmed to room temperature, stirred for 10 h, and refluxed for 5 h more. When dioxane (250 mL) was added to the suspension, a white solid suddenly formed. The resulting suspension was stirred for 10 h and then left to stand for 2 h. The white solid was filtered out, and the

(19) Menage, S.; Vitols, S. E.; Bergerat, P.; Codjovi, E.; Kahn, O.; Girerd, J.-J.; Guillot, M.; Solans, X.; Calvet, T. *Inorg. Chem.* **1991**, *30*, 2666.

(20) Wieghardt, K.; Bossek, K.; Nuber, B.; Weiss, J.; Bonvoisin, J.; Corbella, M.; Vitols, S. E.; Girerd, J.-J. *J. Am. Chem. Soc.* **1988**, *110*, 7398.

(21) Wieghardt, K.; Bossek, K.; Bonvoisin, J.; Beauvillain, P.; Girerd, J.-J.; Nuber, B.; Weiss, J.; Heinze, J. *Angew. Chem., Int. Ed. Engl.* **1986**, *25*, 1030.

(22) Wieghardt, K. *Angew. Chem., Int. Ed. Engl.* **1989**, *28*, 1153.

(23) Böhm, M. C.; Ernst, R. D.; Gleiter, R.; Wilson, D. R. *Inorg. Chem.* **1983**, *22*, 3815.

(24) Theopold, K. N.; Silvester, J.; Byrne, E. K.; Richeson, D. S. *Organometallics* **1989**, *8*, 2001.

(25) Pelter, A.; Smith, K.; Brown, H. C. *Borane Reagents*; Academic: London, 1988; p 227.

(18) van Vleck, J. H. *The Theory of Electric and Magnetic Susceptibilities*; Oxford University Press: Oxford, U.K., 1932.

solution was evaporated to dryness to give a green solid. This solid was dissolved in warm toluene (150 mL) and the small amount of undissolved solid was filtered out while the solution was kept warm. When it was cooled, the solution gave crystals of **1**, which were further recrystallized from hot toluene (58.3%). Anal. Calcd for  $C_{54}H_{66}Mn_3 \cdot C_7H_8$ : C, 75.36; H, 7.68. Found: C, 75.67; H, 7.34. The consistency of the composition of the obtained trimer has been proved (i) by the unit cell determination (the same result) on crystals of five different preparations and (ii) by measuring the magnetic susceptibilities for each crystalline sample used for reactivity studies.

**Synthesis of 2.**  $BPh_3$  (2.59 g, 10.70 mmol) was added to a  $Et_2O$  (400 mL) suspension of **1** (3.50 g, 3.57 mmol). The suspension suddenly became a deep-red solution. Within 30 min, a white solid formed and the red solution turned yellow. The stirring was continued for 12 h at room temperature. The white solid was filtered out and collected (4.7 g, 62.0%). Anal. Calcd for  $C_{45}H_{61}BMnO_3$ : C, 75.52; H, 8.53. Found: C, 75.72; H, 8.63. The mother liquor, analyzed by GC-MS, showed the presence of large amounts of  $BPh_2Mes$ .

**Synthesis of 3.** Complex **1** (13.81 g, 14.0 mmol) was added as a solid to a toluene (400 mL) solution of  $BPh_3$  (21.98 g, 90.0 mmol). The suspension was stirred overnight to give a yellow solution and a white insoluble solid. The suspension was then cooled to  $-15^\circ C$ , and the white solid was collected (10.6 g, 51.2%). Anal. Calcd for  $C_{33}H_{31}BMn$ : C, 80.34; H, 6.33. Found: C, 81.19; H, 6.76. The crystallization solvent (toluene) was lost while drying in vacuo. Crystals suitable for X-ray analysis were obtained from the mother liquor kept at  $3-4^\circ C$  for 3 days. They contain one molecule of toluene of crystallization. The mother liquor was evaporated to dryness and the solid collected with pentane (100 mL). The very small amount of unidentified undissolved solid was filtered out and the yellow solution, analyzed by GC-MS, showed the presence of large amounts of  $BPh_2Mes$ .

**Synthesis of 4.** Complex **1** (3.38 g, 3.47 mmol) was added as a solid to a toluene (100 mL) solution of  $BPh_3$  (10.1 g, 41.7 mmol). The suspension was stirred at room temperature for 2 weeks to give **4** as a light green solid (50%). The mother liquor gave crystals suitable for X-ray analysis. Anal. Calcd for  $C_{60}H_{50}B_2Mn_2 \cdot 1.5C_7H_8$ : C, 81.36; H, 6.00. Found: C, 81.50; H, 6.07.

**X-ray Crystallography for Complexes 1-4.** Suitable crystals of compounds **1-4** were mounted in glass capillaries and sealed under nitrogen. The reduced cells were obtained with the use of TRACER.<sup>26</sup> Crystal data and details associated with data collection are given in Tables 1 and SI (supplementary material). Data were collected at room temperature (295 K) on a single-crystal diffractometer (Philips PW1100 for **1** and Rigaku AFC6S for **2-4**). For intensities and background the "three-point technique" was used for **1**, while individual reflection profiles<sup>27</sup> were analyzed for **2-4**. The structure amplitudes were obtained after the usual Lorentz and polarization corrections,<sup>28</sup> and the absolute scale was established by the Wilson method.<sup>29</sup> The crystal quality was tested by  $\psi$  scans, showing that crystal absorption effects could be neglected for complex **1**. The data for complexes **2-4** were corrected for absorption using a semiempirical method.<sup>30</sup> The function minimized during the least-squares refinement was  $\sum w|\Delta F|^2$  for **1** and **2** and  $\sum w(\Delta F^2)^2$  for **3** and **4**. Weights were

applied according to the scheme  $w = k/\sigma^2(F_o) + g|F_o|^2$  with  $g = 0.005$  and  $0.010$  for complexes **1** and **2**, respectively.<sup>31a</sup> The weighting scheme  $w = 1/[\sigma^2(F_o^2) + (aP)^2]$  ( $P = (F_o^2 + 2F_c^2)/3$ ) was used for **3** and **4**, with  $a = 0.0911$  and  $0.0956$ , respectively.<sup>31b</sup> Anomalous scattering corrections were included in all structure factor calculations.<sup>32b</sup> Scattering factors for neutral atoms were taken from ref 32a for non-hydrogen atoms and from ref 33 for hydrogens. Among the low-angle reflections, no correction for secondary extinction was deemed necessary.

Solutions were based on the observed reflections. Refinement was based on the observed reflections for **1** and **2** using SHELX76<sup>31a</sup> and on the unique total data for **3** and **4** using SHELXL92.<sup>31b</sup> All the structures were solved by the heavy-atom method, starting from three-dimensional Patterson maps. Refinements were first done isotropically and then anisotropically for all non-H atoms, except for the disordered atoms. In complex **2** the C18-C21 carbon atoms of a diethyl ether molecule were found to be disordered over two positions (A and B), which were isotropically refined with site occupation factors of 0.65 and 0.35 for A and B, respectively. During the refinement, the C-O and C-C bond distances of the diethyl ether molecules were constrained to be 1.48(1) and 1.54(1) Å, respectively. In **3**, the toluene solvent molecule of crystallization was affected by disorder, which was solved by considering the molecule to be distributed over two positions (A and B) sharing the C56 carbon atom. The disordered carbon atoms were isotropically refined with a site occupation factor of 0.5 and with constraints imposed on the  $C_{sp^2}-C_{sp^2}$  bond distances (1.395 Å). In complex **4**, one toluene solvent molecule of crystallization was found to be statistically distributed over two positions (A and B); the second toluene molecule was distributed around an inversion center. The disordered carbons were isotropically refined with a site occupation factor of 0.5. During the refinement the aromatic ring of the toluene molecule in complex **1** was constrained to be a regular hexagon (C-C = 1.395 Å).

All the hydrogen atoms, partially found from difference Fourier maps and partially put in geometrically calculated positions, were introduced in the final refinement as fixed-atom contributions with isotropic  $U$ 's fixed at  $0.12 \text{ \AA}^2$  for **1** and **2** and equal to 1.2 times the  $U_{eq}$  value of the corresponding carbon atom for **3** and **4**. The hydrogens related to the disordered ethyl groups in **2** and to the toluene molecules in **3** and **4** were ignored. The final difference maps showed no unusual features, with no significant peak having chemical meaning above the general background. Final atomic coordinates are listed in Tables 2-5 for non-H atoms and in Tables SII-SV (supplementary material) for hydrogens. Thermal parameters are given in Tables SVI-IX and bond distances and angles in Tables SX-XIII (supplementary material).<sup>34</sup>

**Magnetic Measurements for Complexes 1, 3, and 4.** Magnetic susceptibility measurements were made on a MPMS5 SQUID susceptometer (Quantum Design Inc.) operating at a magnetic field strength of 3 kG. Corrections were applied for diamagnetism calculated from Pascal constants. Effective magnetic moments were calculated by the equation  $\mu_{eff} = 2.828(\chi_{Mn}T)^{1/2}$ , where  $\chi_{Mn}$  is the magnetic susceptibility per manganese. Variable-field magnetization data were measured on the same susceptometer at 1.9 and 6.0 K, in the range 3-55 kG. Fitting of the magnetic data to the theoretical expression

(26) Lawton, S. L.; Jacobson, R. A. TRACER (a Cell Reduction Program); Ames Laboratory, Iowa State University of Science and Technology: Ames, IA, 1965.

(27) Lehmann, M. S.; Larsen, F. K. *Acta Crystallogr., Sect. A: Cryst. Phys., Diff., Theor. Gen. Crystallogr.* **1974**, *A30*, 580-584.

(28) Data reduction, structure solution, and refinement were carried out on an IBM AT personal computer equipped with an Inmos T800 transputer and on an Encore 91 computer.

(29) Wilson, A. J. C. *Nature* **1942**, *150*, 151.

(30) North, A. C. T.; Phillips, D. C.; Mathews, F. S. *Acta Crystallogr., Sect. A: Cryst. Phys., Diff., Theor. Gen. Crystallogr.* **1968**, *A24*, 351.

(31) (a) Sheldrick, G. M. SHELX-76: Program for Crystal Structure Determination; University of Cambridge, Cambridge, U.K., 1976. (b) Sheldrick, G. M. SHELXL-92. Program for crystal structure refinement. University of Göttingen, Göttingen, Germany, 1992.

(32) (a) *International Tables for X-ray Crystallography*; Kynoch Press: Birmingham, U.K., 1974; Vol. IV, p 99. (b) *Ibid.*, p 149.

(33) Stewart, R. F.; Davidson, E. R.; Simpson, W. T. *J. Chem. Phys.* **1965**, *42*, 3175.

(34) See paragraph at the end of the paper regarding supplementary material.

were performed by minimizing the agreement factor, defined as

$$R = \sum \frac{[\chi_i^{\text{obsd}}T - \chi_i^{\text{calcd}}T]^2}{(\chi_i^{\text{obsd}}T)^2}$$

through a Levenberg–Marquardt routine.<sup>35</sup>

**Acknowledgment.** We thank the “Fonds National Suisse de la Recherche Scientifique” (Grant No. 20-

(35) Press, W. H.; Flannery, B. P.; Teukolsky, S. A.; Vetterling, W. T. *Numerical Recipes*; Cambridge University Press: Cambridge, U.K., 1989.

40268.94), Ciba-Geigy Co. (Basel, Switzerland), and Action COST D3 (European Program for Scientific Research) for financial support.

**Supplementary Material Available:** Tables of experimental details associated with data collection and structure refinement (Table SI), hydrogen atom coordinates (Tables SII–SV), thermal parameters (Tables SVI–SIX), and bond distances and angles (Tables SX–SXIII) for 1–4 (21 pages). Ordering information is given on any current masthead page.

OM940977A